

- amounts of certain other gene products are reduced by 50% (J. A. Fischer-Vize, unpublished data). One *Hs-faf<sup>Ser1677</sup>* line was tested for dominant-negative activity in a *faf<sup>FO8</sup>/faf<sup>BX3</sup>* background by heat shocking transformant larvae as described (11), but no increase in eye roughness was ever observed.
14. M. Glotzer, A. W. Murray, M. W. Kirschner, *Nature* **349**, 132 (1991); R. J. Deshaies, V. Chau, M. W. Kirschner, *EMBO J.* **14**, 303 (1995); J. Yaglom *et al.*, *Mol. Cell. Biol.* **15**, 731 (1995).
  15. M. Treier, L. M. Staszewski, D. Bohmann, *Cell* **78**, 787 (1994); D. Kornitzer, B. Raboy, R. G. Kulka, G. R. Fink, *EMBO J.* **13**, 6021 (1994); V. J. Palombella, O. J. Rando, A. L. Goldberg, T. Maniatis, *Cell* **78**, 773 (1994).
  16. K. L. Rock *et al.*, *Cell* **78**, 761 (1994).
  17. M. G. Muralidhar and J. B. Thomas, *Neuron* **11**, 253 (1993); C. E. Oh, R. McMahon, S. Benzer, M. A. Tanouye, *J. Neurosci.* **14**, 3166 (1994).
  18. G. Sambrook, E. F. Fritsch, T. Maniatis, *Molecular Cloning: A Laboratory Manual* (Cold Spring Harbor Laboratory, Cold Spring Harbor, NY, 1989).
  19. C. S. Thummel and V. Pirota, *Dros. Inf. Serv.* **71**, 150 (1992).
  20. Abbreviations for the amino acid residues are A, Ala; C, Cys; D, Asp; E, Glu; F, Phe; G, Gly; H, His; I, Ile; K, Lys; L, Leu; M, Met; N, Asn; P, Pro; Q, Gln; R, Arg; S, Ser; T, Thr; V, Val; W, Trp; and Y, Tyr.
  21. H. I. Miller *et al.*, *Biotechnology* **7**, 698 (1989); K. D. Wilkinson *et al.*, *Science* **246**, 670 (1989); N. Zhang, K. Wilkinson, M. Bownes, *Dev. Biol.* **157**, 214 (1993).
  22. Site-directed mutagenesis was performed with oligonucleotides and single-stranded DNA templates (subclones of an ~0.7-kb Hpa I-Kpn I genomic DNA fragment containing the Cys domain and an ~2.0-kb Kpn I-Sph I fragment containing the His domain) by means of standard techniques (18). To ensure that no other mutations were introduced, we determined the entire DNA sequence of each mutagenized fragment before reconstituting the ~13-kb *faf* genomic DNA fragment. Oligonucleotides (Integrated DNA Technologies Inc., Coralville, IA) used for the mutagenesis (mutagenic residues are in bold) were 5'-CAGGTGCCACTTC-CTACATGAATTC-3' (Cys<sup>1677</sup>→Ser), 5'-GCCTGTC-CGCTCGCACCACAAATGC-3' (His<sup>1959</sup>→Arg), and 5'-TAACTGAAGTAGCGACCCGCCGAAG-3' (His<sup>1967</sup>→Arg). The mutant *faf* genes were cloned as Not I fragments into the P element transformation vector Casper3 (19), and P element transformants were generated in the strain *w<sup>1118</sup>* as described [A. C. Spradling, in *Drosophila: A Practical Approach*, D. B. Roberts, Ed. (IRL Press, Oxford, 1986), pp. 175–197].
  23. The average fraction of wild-type facets for each transformant line was calculated by counting 300 to 1300 facets in two to six eyes for each line. The variation between eyes within a given genotype was significant only for the *faf<sup>Arg1959</sup>* and *faf<sup>Arg1967</sup>* lines. All of the transformant lines contained two copies of the P element except for two *faf<sup>Ser1677</sup>* lines and one *faf<sup>Arg1967</sup>* line, which contained one copy each (these gave nonexceptional results). In all but one case, all three *faf* mutant facet phenotypes (Fig. 2, D to F) were present in the lines containing the mutant *faf* gene, indicating that the sole function of FAF in the eye is as a Ubp. Some transformant lines partially rescue the *faf<sup>BX4</sup>* eye phenotype, probably because Ser and Arg can substitute functionally (although poorly) for Cys and His, respectively. Thus, rescue likely occurs in the lines that express the most mutant FAF protein. In all cases, female transformants remained sterile in a *faf<sup>BX4</sup>* background.
  24. Sectioning and photography were performed as described [A. Tomlinson and D. F. Ready, *Dev. Biol.* **123**, 264 (1987)]. For scanning electron micrographs (SEMs), flies were dehydrated in ethanol, critical-point-dried in carbon dioxide, sputter-coated, and photographed with a Philips 515 scanning electron microscope.
  25. T. Wolff and D. F. Ready, in *The Development of Drosophila melanogaster*, M. Bate and A. Martinez-Arias, Eds. (Cold Spring Harbor Laboratory Press, Cold Spring Harbor, NY, 1993), vol. 2, chap. 22.
  26. Suppression was quantitated by calculating the fraction of wild-type facets in the eyes of *faf<sup>FO8</sup>/faf<sup>FO8</sup>* and *l(3)73Ai<sup>1</sup> faf<sup>FO8</sup>/ + faf<sup>FO8</sup>* flies: 495 facets in sections of two *faf<sup>FO8</sup>/faf<sup>FO8</sup>* eyes and 981 facets in four *l(3)73Ai<sup>1</sup> faf<sup>FO8</sup>/ + faf<sup>FO8</sup>* eyes were counted, and 6.5% versus 65% wild-type facets were found, respectively. Similar results were obtained with two other alleles of *l(3)73Ai* [*l(3)73Ai<sup>1</sup>rv10e* and *l(3)73Ai<sup>1</sup>rv22e*; unpublished alleles obtained from J. Belote].
  27. Embryos were collected on plates for 20 hours; the plates were put in a 37°C incubator for 1.5 hours and then at room temperature for 4 to 5 hours. Embryo extracts were then prepared as described [S. Misra and D. Rio, *Cell* **62**, 269 (1990)], quantitated with the Bio-Rad protein assay, and 200 µg of protein per lane was run on a 5% SDS acrylamide gel. Electrophoresis and transfer to nitrocellulose were according to standard procedures (18). The blot was developed with a monoclonal antibody to the Myc epitope (cell supernatant from 9E10.2 cells; American Type Culture Collection, Rockville, MD) and alkaline phosphatase-conjugated secondary antibody to mouse immunoglobulin G (Vector Laboratories, Burlingame, CA) with an alkaline phosphatase substrate kit (Vector Laboratories).
  28. The wild-type *faf* cDNA was assembled by joining cDNAs 3-2 and 7-3 (8) and thus encoded the form of FAF protein that uses the most 5' TAG (Fig. 1A). Before assembly, annealed oligonucleotides (Integrated DNA Technologies) containing the Myc epitope [P. A. Kolodziej and R. A. Young, *Methods Enzymol.* **194**, 508 (1994)] within Xho I ends (5'-TCGAGGATCCCCCGAGCAGAGAGCTGATCTC-CGAGGAGGACCTGAAC-3' and 5'-TCGAGTTCA-GGTCTCTCTCGGAGATCAGCTCTGCTCGGGG-GGGATCC-3') were inserted into an Xho I site in the *faf* cDNA, which resulted in the addition of 16 amino acids (RTPPEQKLISEEDLNS) (20) between Ser<sup>63</sup> and Ser<sup>64</sup> in FAF (8). The assembled wild-type *faf* cDNA was cloned as an Asc I fragment into pB-Shsp-(N2-A)pa, a modified form of pBShsp that contains heat shock promoter sequences (10) and the simian virus 40 (SV40) polyadenylation site from pC4βgal [C. S. Thummel, A. M. Boulet, H. D. Lipshitz, *Gene* **74**, 543 (1988)] separated by an Asc I site. The entire hybrid gene was then cloned into the P-element transformation vector Casper3 (19) as a Not I fragment. The *Hs-faf<sup>Ser1677</sup>* gene was constructed the same way except that a 0.7-kb Hpa I-Kpn I fragment of genomic DNA containing the Ser<sup>1677</sup> mutation was substituted for the wild-type cDNA fragment.
  29. A 2.2-kb Bam HI-Sph I fragment of wild-type or mutant *faf* cDNA (see Fig. 3) was subcloned into pQE30 (Qiagen, Inc., Chatsworth, CA) to produce the pQE-FAF or pQE-FAF<sup>Ser1677</sup>, respectively. Iso-propyl-β-D-thiogalactopyranoside induction produced an abundant protein of the expected size (84 kD) from each plasmid.
  30. We thank J. Belote for the *l(3)73Ai* alleles, J. Mendenhall and the University of Texas, Austin, Cell Research Institute for the SEMs, S. Olivelle and the University of Texas, Austin, Hybridoma Center for preparing the anti-Myc supernatant, J. Loera for fly culture media, G. Gage and J. Young for preparation of Figs. 2 and 3, M. Simon for pBShsp, and M. Hochstrasser and everyone in our laboratories for stimulating discussions. Supported by grants from the NIH and the Molecular Biology Institute at the University of Texas, Austin (J.A.F.-V.), by a grant from the Australian Capital Territory Cancer Society (R.T.B.), and by an Australian Research Council QEII Fellowship (R.T.B.).

2 August 1995; accepted 16 October 1995

## Precise Spatial Positioning of Chromosomes During Prometaphase: Evidence for Chromosomal Order

Robert Nagele,\*† Theresa Freeman,\* Lydia McMorow, Hsin-yi Lee

The relative locations of several chromosomes within wheel-shaped prometaphase chromosome rosettes of human fibroblasts and HeLa cells were determined with fluorescence hybridization. Homologs were consistently positioned on opposite sides of the rosette, which suggests that chromosomes are separated into two haploid sets, each derived from one parent. The relative locations of chromosomes on the rosette were mapped by dual hybridizations. The data suggest that the chromosome orders within the two haploid sets are antiparallel. This chromosome arrangement in human cells appears to be both independent of cell type- and species-specific and may influence chromosome topology throughout the cell cycle.

Studies with fluorescence in situ hybridization (FISH) have increased our understanding of the structural and functional organization of the cell nucleus (1, 2). At interphase, individual chromosomes occupy

compact, discrete territories. The specific structure and location of these chromosome territories may be specific for both cell type and stage of the cell cycle (3). For example, in cells of the human and mouse central nervous system, specific chromosomal domains are organized in a reproducible manner (4). In human fibroblasts, chromosome 8 centromeric regions are distributed non-randomly, and the distribution changes during the cell cycle, such that the chromosomes are situated peripherally with arms extending toward the nuclear interior at G<sub>1</sub> but are more centrally located with arms

R. Nagele and T. Freeman, Department of Molecular Biology, University of Medicine and Dentistry of New Jersey, School of Osteopathic Medicine, Stratford, NJ 08084, USA.

L. McMorow, Department of Laboratory Science, Thomas Jefferson University, Philadelphia, PA 19107, USA. H.-y. Lee, Department of Biology, Rutgers University, Camden, NJ 08102, USA.

\*These authors contributed equally to this work.

†To whom correspondence should be addressed.

extending toward the nuclear periphery at  $G_2$  (5, 6). Chromosome 1 centromeric DNA is restricted to the nuclear periphery in hematopoietic cells (7). The centromere and telomere distribution patterns in interphase nuclei appear to be dependent on both cell type and stage of the cell cycle, and may be influenced by the state of cell differentiation (2, 6, 8–10).

We have now investigated the possibility that there is an underlying spatial organization of chromosome territories in all somatic cells of a given species. We have

taken advantage of the fact that all human chromosomes at prometaphase are aggregated briefly into a single, wheel-shaped ring known as the chromosome rosette (Fig. 1, A to D). If cells possess an inherent spatial order of chromosomes, the specific arrangement of chromosomes on the rosette should consistently reflect this precise order. To explore this possibility, we examined the relative spatial arrangement of chromosome homologs in prometaphase rosettes of two types of normal human diploid fibroblasts (HDFs), derived from

skin and lungs, and HeLa cells (11) with FISH (12) and chromosome-specific DNA probes [alpha-satellite and whole chromosome painting probes (13)] (Fig. 1). The nuclei of these cells are well suited for this type of analysis because they are flattened against the substratum during much of the cell cycle, such that the intranuclear arrangement of chromosome domains appears nearly two-dimensional. This two-dimensional geometry of HDFs and HeLa cells enables direct microscopic examination of the full complement of radially arranged chromosomes and allows most fluorescence signals that emanate from flat nuclei to be observed and recorded photographically from a single focal plane, greatly facilitating analysis and interpretation of signal distribution patterns. At the hub of the rosette, chromosomes are aligned with one another at the level of their centromeric subdomains, such that, in FISH preparations with a DNA probe for all human centromeres (14), closely juxtaposed centromeres often appear as a single fluorescent ring (Fig. 1, A and B). Most chromosomes within the rosette are oriented such that their arms project outward from the region of the centromere ring, leaving the hub of the rosette virtually devoid of chromatin and generating a wreath-like appearance (Fig. 1, A to D and T). Chromosome rosettes form rapidly, exist only briefly, and are oriented horizontally (that is, parallel to the culture substratum). HDFs display well-formed, horizontal rosettes at prometaphase for only 5 to 10 min of their total cell cycle time of 30 hours. Thus, only 0.28 to 0.56% of total cells are expected to display fully formed prometaphase rosettes at any given time.

To determine whether chromosomes in human cells are in a consistent spatial order

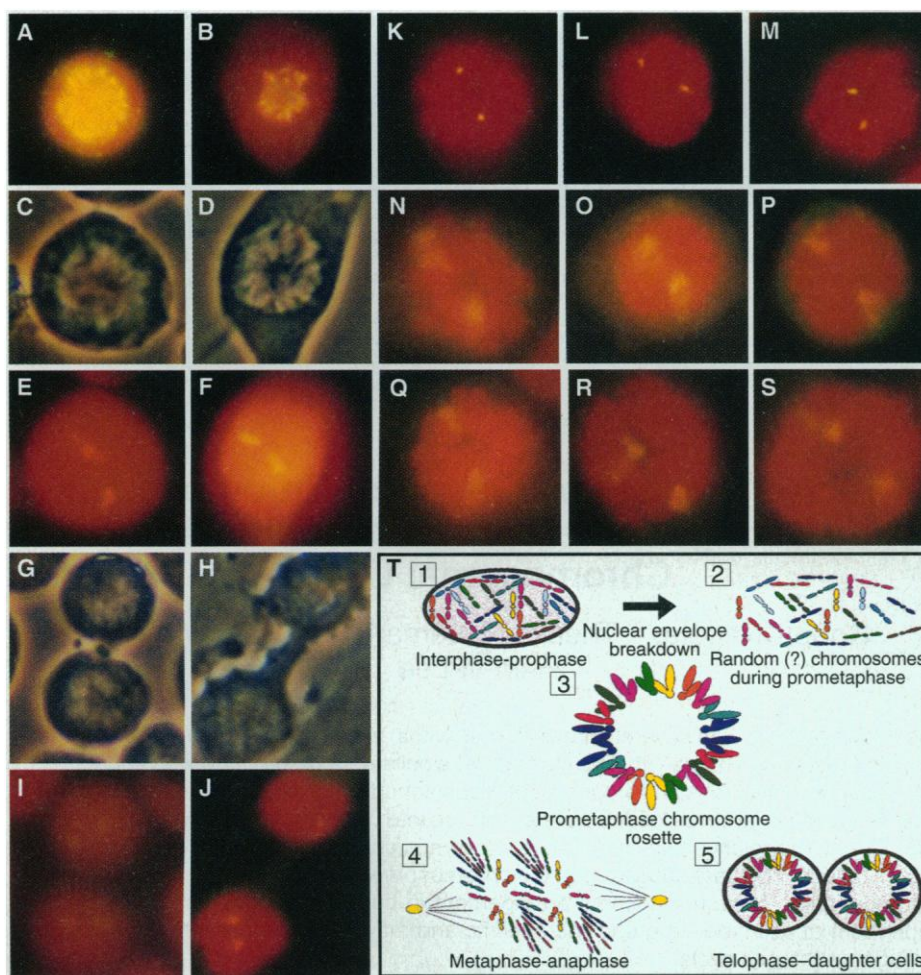


**Fig. 1.** Mapping of the relative spatial locations of chromosomes 7, 8, 16, and X in the chromosome rosettes of HDFs and HeLa cells with FISH and digoxigenin-labeled chromosome-specific DNA probes (12). In FISH images, the digoxigenin-labeled probe appears yellow against a reddish-orange background counterstaining with propidium iodide. (A and B) The location of centromeric subdomains in prometaphase HeLa cells and HDFs, respectively, revealed by hybridization with a DNA probe for all human centromeres (14). Centromeres are closely juxtaposed at the hub of the chromosome rosette and appear as a single fluorescent ring. (C and D) Phase-contrast images of horizontal, wheel-shaped rosettes of prometaphase chromosomes of HeLa cells and HDFs, respectively, showing a radial chromosome arrangement around a central region that is largely devoid of chromatin. (E and F) Localization of chromosome 16 in the same cells as in (C) and (D), showing the two homologs positioned on opposite sides of the prometaphase rosette. (G to J) Phase-contrast and FISH images of HeLa cells (G and I) and HDFs (H and J) during cytokinesis, showing that chromosome 16 homologs remain on opposite sides of the chromosome rosette throughout mitosis. (K to S) FISH images showing the locations of the homologs of chromosome X (K, L, and M) (with an alpha-satellite probe) and chromosomes 7 (N, O, and P) and 8 (Q, R, and S) (with whole-chromosome painting probes) on opposite sides of the prometaphase chromosome rosette of HDFs. Magnification,  $\times 1130$  (A to S). (T) Schematic model depicting the proposed precise spatial arrangement of chromosomes in human cells and the means by which chromosome order may be transmitted from one cell generation to the next.

**Table 1.** Quantitation of the relative positions of chromosome homologs in prometaphase chromosome rosettes of HDFs (15). The angular separation of homologs on each circular rosette was measured in degrees. Each rosette encompassed  $360^\circ$ , and the exact center of the rosette was used as a reference point. Data were pooled from two types of fibroblasts, Detroit 551 and CCD-34Lu, derived from human skin and lungs, respectively. Data for chromosomes 1 and 9 were obtained from chromosome rosettes of nocodazole-treated HDFs. Values are means  $\pm$  SD.

Chromosome	Angular separation (degrees)	n
7	$144 \pm 21.5$	36
8	$148 \pm 24.7$	46
16	$145 \pm 22.8$	42
X	$153 \pm 25.4$	22
9	$150 \pm 25.3$	13
1	$166 \pm 16.0$	8



within the prometaphase chromosome rosette, we mapped the relative spatial locations of several selected sets of chromosome homologs with FISH and chromosome-specific DNA probes (13) (Fig. 1, E to S). Selection criteria for cells studied included a well-formed, circular chromosome rosette free from structural distortion, a radial chromosome array, and the presence of the expected number of fluorescence signals (one for each homolog). Although these criteria were relatively stringent, we aimed to minimize the possibility that spatial interrelations among chromosomes within the rosette might be misinterpreted or remain undetected because of artifactual variations in the position of chromosome homologs. Thus, only ~20% of prometaphase chromosome rosettes were included in this study.

Figure 1 (E and F and K to S) shows representative well-formed, circular rosettes of prometaphase chromosomes subjected to FISH with whole chromosome painting probes for chromosomes 7, 8, and 16 and an alpha-satellite probe for chromosome X in HDFs, and with a painting probe for chromosome 16 in HeLa cells. Chromosome homologs were invariably positioned on opposite sides of the rosette. To quantitate the relative spatial positions of chromosome homologs on rosettes, we measured their

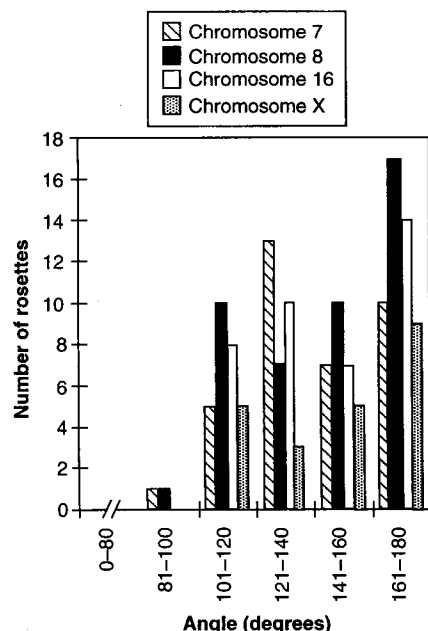


**Fig. 2.** Relative positions of chromosome homologs on the prometaphase chromosome rosettes of HDFs. The distribution of measured angular separations of homologs of chromosomes 7, 8, 16, and X on the circular chromosome rosettes of HDFs, with each wheel-like rosette encompassing 360° and the center of the rosette taken as the reference point (15), is shown. Homologs were never found within 90° of each other on the rosette, suggesting that one homolog is restricted to each half of the rosette.

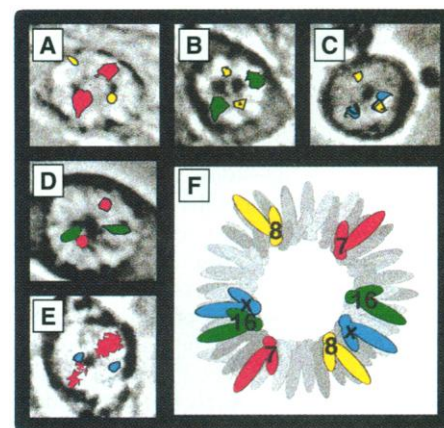
angular separation, with each wheel-like rosette encompassing 360° and with the exact center of the rosette as the reference point (15). The mean angular separation of homologs was similar (range, 144° to 166°) for chromosomes 1, 7, 8, 9, 16, and X (Table 1). The distribution of measured angular separation of homologs (range 144° to 153°) for chromosomes 7, 8, 16, and X is shown in Fig. 2. Homologs were never situated within 90° of each other on the rosette, whereas a random distribution would predict homologs to be positioned within 90° of each other in 50% of rosettes. Thus, chromosome homologs are prevented from being in close proximity to one another and are positioned with one homolog in each half of the rosette. This spatial relation among chromosome homologs remained constant even with variations in the diameter of the rosette (16, 17). Furthermore, analysis of the relative spatial positioning of chromosomes 1 and 9 in rosettes of nocodazole-treated HDFs (11) yielded mean angular separations of 166° and 150°, respectively (Table 1), consistent with results for chromosomes 7, 8, 16, and X in untreated cells. Nocodazole was used to arrest cells in prometaphase, thereby increasing the fraction of cells displaying well-formed prometaphase chromosome rosettes (18). Apparently, nocodazole has no effect on the formation of the chromosome rosettes or on the spatial distribution of chromosomes within it. However, because cells are arrested in prometaphase for a prolonged period, chromosome compaction appears to continue during this interval and results in a progressive decrease in the diameter of rosettes (16).

The observation that cells exhibit consistent distribution patterns of chromosome

homologs situated on opposite sides of the chromosome rosette essentially eliminates the possibility that the patterns are an artifact or occurred by chance. In addition, examination of cells at telophase and during cytokinesis revealed that chromosomes remain arranged in a compact rosette configuration, and that the spatial positioning of homologs on opposite sides of the rosette is preserved throughout the remainder of mitosis (Fig. 1, G to J and T). Thus, a consistent spatial arrangement of chromosome homologs exists on the prometaphase rosettes of human HDFs and HeLa cells (Fig. 1T) and may indicate that all 46 chromosomes are arranged similarly in human cells (19). Because rosettes from both human skin and lung fibroblasts and HeLa cells exhibit similar chromosome distribution patterns, the spatial arrangement of chromosome homologs on opposite sides of prometaphase rosettes appears to be both independent of cell type and species specific. In addition, our data suggest that chromosomes on the rosette are separated into two distinct groups of 23 different homologs, with each "haploid chromosome set" presumably derived from one parent. Although the exact order of all chromosomes within the rosette and each haploid chromosome set remains to be determined, the positioning of chromosome homologs on opposite sides of the rosette suggests an antiparallel order. An antiparallel chromosome arrangement would require nonhomologous chromosomes to maintain a constant spatial relation with respect to each other within each half of the rosette.

To test for antiparallel chromosome order, we performed dual hybridizations with prometaphase chromosome rosettes of HDFs and the following combinations of chromo-

**Fig. 3.** Mapping of the relative spatial order of chromosomes 7, 8, 16, and X on prometaphase chromosome rosettes of HDFs by FISH with combinations of digoxigenin-labeled DNA probes (20). (A to E) Fluorescence signals from chromosome homologs are superimposed over phase-contrast images of the same cell. The relative distributions of chromosomes 7 and 8 (A), 8 and 16 (B), 8 and X (C), 7 and 16 (D), and 7 and X (E) further confirm the positioning of homologs on opposite sides of the rosette and show the spatial relation of the different chromosomes within each half of the rosette. Magnification,  $\times 1130$  (A to E). (F) Diagram summarizing chromosome distribution patterns on the prometaphase chromosome rosette obtained from dual hybridizations of >30 rosettes. The relative spatial order of chromosomes 7, 8, 16, and X on each half of the rosette is consistent with an antiparallel chromosome arrangement. Chromosomes 16 and X were closely associated on both sides of the rosette, whereas the positions of chromosomes 7 and 8, relative to X and 16, were more variable. Although this variability may be due to subtle differences in the geometry of chromosome rosettes as well as to local changes in the degree of chromosome compaction, the possibility cannot be excluded that the antiparallel order is only generalized and therefore may not be identical (that is, a mirror image) on each half of the rosette for all chromosomes.



some-specific alpha-satellite probes and whole chromosome painting probes (13): chromosomes 7 and 8, 8 and 16, 8 and X, 7 and 16, and 7 and X (Fig. 3) (20). Our goal was to determine the relative spatial order of these four chromosomes within each half of the rosette by analysis of superimposed FISH images. Results obtained from images of >30 HDF prometaphase rosettes revealed the relative order of chromosomes 7, 8, 16, and X, and the results are consistent with an anti-parallel arrangement of chromosomes on the rosette for each set of individual homologs (21). We propose that this chromosome arrangement originates from fusion of maternal and paternal haploid chromosome sets at the time of fertilization and that a precise spatial order of chromosomes may be a common feature in eukaryotic cells.

The mechanism by which a consistent spatial order of chromosomes is achieved and maintained within the rosette is unknown. One possibility is that chromosomes are attached permanently to one another in a precise order at the level of their centromeric domains. Although centromeric interconnections have not yet been observed, the tendency for centromeres to line up into a "string of pearls" arrangement during  $G_2$  (9, 10, 22) and to form a ring at the hub of the prometaphase rosette (Fig. 1, A and B) provides indirect support for their existence (23). Permanent associations among adjacent chromosomes would be expected to influence chromosome topology in the interphase nucleus, and adjacent interconnected chromosomes would remain in relatively close proximity throughout the cell cycle, thereby linking the spatial positioning of chromosomes in the prometaphase rosette with that in interphase nuclei. Chromosomes 16 and X are closely juxtaposed on the prometaphase chromosome rosette (Fig. 3F), and examination of interphase HDF nuclei has revealed that homologs of chromosome 16 are indeed positioned adjacent to those of chromosome X in most nuclei (24). Centromeric interconnections would also eliminate randomness of chromosome congression movements toward the forming metaphase plate, ensure that all chromosomes are incorporated into the chromosome rosette by the end of prometaphase, and help to maintain the remarkable success rate of mitosis (individual chromosomes that may not have attached to spindle microtubules might still be segregated properly because of their link to neighboring chromosomes).

A consistent, cell type-independent chromosome arrangement in human cells may also have direct relevance to the mechanisms of chromosomal translocation. Thus, the high frequencies of translocations among certain chromosomes may be related

to the fact that they are adjacent to one another on the chromosome rosette, which may prove to have a significant effect on the etiology of certain cancers that are thought to arise, at least in part, through genetic errors that accompany chromosome translocations. Lastly, the existence of a precise chromosome order in normal human cells may provide insight into the mechanisms of aneuploidy and stable transmission of the aneuploid condition from one cell generation to another. For example, it is conceivable that aneuploidy is mediated in part by stable incorporation of extra chromosomes or small groups of interconnected chromosomes into the chromosome rosette. Our observation that chromosomes are assembled into a single, well-formed rosette in two types of aneuploid human cells—HeLa cells and K562 erythroleukemia cells (25)—supports this possibility. In addition, the similar spatial arrangement of chromosome 16 in both normal cells (HDFs) and aneuploid cells (HeLa) suggests that some chromosomes maintain their normal spatial order in aneuploid cells.

## REFERENCES AND NOTES

1. L. Manuelidis, *Proc. Natl. Acad. Sci. U.S.A.* **81**, 3123 (1984); *Hum. Genet.* **71**, 288 (1985); M. Hochstrasser, D. Mathog, Y. Gruenbaum, H. Saumweber, J. Sedat, *J. Cell Biol.* **102**, 112 (1986); T. Cremer, P. Lichter, J. Borden, D. Ward, L. Manuelidis, *Hum. Genet.* **80**, 235 (1988); P. Lichter, T. Cremer, J. Borden, L. Manuelidis, D. Ward, *ibid.*, p. 224; J. Landegent *et al.*, *Proc. Natl. Acad. Sci. U.S.A.* **85**, 9138 (1988); A. Hilliker and R. Appels, *Exp. Cell Res.* **185**, 297 (1989).
2. C. Vourch, D. Taruscio, A. Boyle, D. Ward, *Exp. Cell Res.* **205**, 142 (1993).
3. For reviews, see L. Manuelidis, *Science* **250**, 1533 (1990); T. Haaf and M. Schmid, *Exp. Cell Res.* **192**, 325 (1991); R. Hulsas and J. Bauman, *Cell Biol. Int. Rep.* **16**, 739 (1992); D. Spector, *Annu. Rev. Cell Biol.* **9**, 265 (1993).
4. L. Manuelidis and J. Borden, *Chromosoma* **96**, 397 (1988).
5. S. Popp *et al.*, *Exp. Cell Res.* **189**, 1 (1990).
6. M. Ferguson and D. Ward, *Chromosoma* **101**, 557 (1992).
7. H. Van Dekken *et al.*, *Cytometry* **11**, 570 (1990).
8. L. Manuelidis, *Ann. N.Y. Acad. Sci.* **450**, 205 (1985); G. Hadlaczy, M. Went, N. Ringertz, *Exp. Cell Res.* **167**, 1 (1986); H. Funabiki, I. Hagan, S. Uzawa, M. Yanigida, *J. Cell Biol.* **121**, 961 (1993); J. Janeski, P. Park, U. DeBoni, *Exp. Cell Res.* **217**, 227 (1995).
9. T. Haaf and R. Schmid, *Hum. Genet.* **81**, 137 (1989).
10. M. Bartholdi, *J. Cell Sci.* **99**, 255 (1991).
11. Human diploid skin and lung fibroblasts (Detroit 551 and CCD-34Lu, respectively; American Type Culture Collection) were grown as monolayers on glass cover slips in Dulbecco's modified Eagle's medium (DMEM) (Gibco) containing 10% fetal bovine serum (FBS) (Gibco) and 1% penicillin-streptomycin at 37°C in a 5% CO<sub>2</sub> atmosphere. Some cultures were treated with nocodazole (40 ng/ml) (Sigma) for 4 to 12 hours to arrest cells at prometaphase. Cells were washed gently in Hanks' balanced salt solution (HBSS), fixed with 4% paraformaldehyde in phosphate-buffered saline (PBS) [137 mM NaCl, 3 mM KCl, 16 mM Na<sub>2</sub>HPO<sub>4</sub>, 2 mM KH<sub>2</sub>PO<sub>4</sub> (pH 7.3)] for 20 min at room temperature, and either prepared immediately for FISH or dehydrated in a graded series of increasing concentrations (30, 50, 70, and 95%, 5 min each) of cold (4°C) ethanol and stored in 95% ethanol at -20°C until use. HeLa S3 cells were cultured at 37°C in DMEM supplemented with 10% FBS, 4 mM glutamine, penicillin (100 U/ml), and streptomycin (0.1 mg/ml). Mitotic cells were obtained by selective detachment, washed in HBSS, resuspended in 4% paraformaldehyde in PBS, and immediately attached to microscope slides with a Cytospin (Shandon Southern Instruments) at 500g for 5 min. Fixation of cells was then continued for an additional 15 min.
12. FISH was performed with cells on glass cover slips essentially as described (2) with digoxigenin-labeled probes. Detection was performed with fluorescein isothiocyanate-conjugated sheep antibodies to digoxigenin (200 µg/ml) (Boehringer Mannheim) for 20 min at 37°C. Cover slips were mounted in Vectashield antifade mounting solution (Vector) containing propidium iodide (200 ng/ml) as a counterstain. Controls for FISH included hybridization without labeled probe or omission of the detection reagent that binds to the probe. Slides were stored at 4°C until use. Specimens were examined with a Nikon Optiphot microscope equipped with epifluorescence optics, a SIT-66 video camera, and a Dage 100 digital image processor. For most photographs, a ×60 objective with a numerical aperture of 1.40 was used in combination with a ×4.0 photo eye piece for a total magnification of ×240 at the camera. Fluorescence images were recorded on either Kodak T-Max 400 negative film or Fuji-chrome 400 color film.
13. Whole chromosome painting probes (Coatasome 7, Coatasome 8, and Coatasome 16; Oncor) and alpha-satellite probes specific for chromosomes X, 1, and 9 (Oncor) were prepared for hybridization according to the recommendations of the manufacturer and used as described (12).
14. The DNA probe for all human centromeres (Oncor) comprises a selection of sequences that targets the centromeric subdomains of all human chromosomes.
15. Measurement of the angular separation between homologs was preferable to that of actual distances because rosettes vary in diameter, presumably reflecting individual differences in the overall degree of chromosome compaction during prometaphase. Measurements of the angular separation of chromosome homologs on each circular rosette satisfying the selection criteria were performed directly on projected photographic negative images. The center of the rosette was used as a reference point, and the angle between homologs was measured. With this method, a maximal spatial separation of homologs would be 180°, where homologs would be positioned exactly on opposite sides of the rosette. For specimens treated with whole chromosome painting probes and for which fluorescence signals were relatively large and diffuse, the line drawn from the central reference point of the rosette and passing through the exact center of the fluorescent chromosome territory was taken to represent the position of that chromosome homolog. Fluorescence signals from chromosome-specific alpha satellites were small and punctate and were considered to represent the position of the chromosome homolog. Measurements of chromosome position on prometaphase chromosome rosettes were generally more accurate in cells hybridized with chromosome-specific alpha-satellite probes because fluorescence signals were more intense, highly localized and positioned at the hub of the rosette. In cells hybridized with whole chromosome painting probes, chromosome arms sometimes radiated at an acute angle from the centromeric region at the hub of the rosette (Fig. 1Q), resulting in some variability in the apparent location of the chromosome.
16. Despite having an overall circular shape, chromosome rosettes at prometaphase exhibit variations in diameter that are thought to reflect individual variation in the degree of chromatin compaction within chromosomes. The diameter of prometaphase rosettes was 14.4 ± 2.1 µm (mean ± SD; n = 58) in HDFs and 12.4 ± 1.0 µm (n = 20) in HeLa cells. The diameter of prometaphase rosettes in nocodazole-treated HDFs [12.4 ± 1.8 µm (n = 40)] was slightly smaller than that in untreated HDFs.

17. Examination of rosettes subjected to FISH with whole chromosome painting probes revealed that individual chromosome domains are too wide for the structure of the rosette to be in the form of a monolayer. Measurements of the territorial widths of chromosomes 7 and 16 allow for only 16 to 20 chromosomes to complete the full circle of the rosette as a monolayer, suggesting that the arrangement of chromosomes within rosettes is either multilayered or pseudo-multilayered (staggered). In either instance, the packing strategy is likely to introduce variability in the measured spatial separation of chromosomes. Analysis of the three-dimensional arrangement of chromosomes and their centromeric subdomains at the hub of the rosette by confocal or serial-section electron microscopy should clarify this issue.
18. M. Jordan, D. Thrower, L. Wilson, *J. Cell Sci.* **102**, 401 (1992).
19. In rosettes not included in this study because they did not satisfy the selection criteria, homologs were virtually always positioned on opposite sides of the rosette. Detectable deviations from this precise spatial positioning were often clearly associated with local structural distortions of the rosette, and in many of these instances, visual compensation for obvious structural distortions resulted in the typical homolog distribution pattern.
20. Dual hybridizations with combinations of chromosome-specific alpha-satellite probes and whole-chromosome painting probes were performed on prometaphase chromosome rosettes of HDFs to determine the relative spatial order of chromosomes 7, 8, 16, and X. Hybridization conditions were optimized to facilitate detection of signals emanating from both probes. The spatial order of chromosome homologs was determined by superposition of multiple FISH images representing each dual hybridization over the corresponding phase-contrast image with the use of COREL graphics software.
21. Despite the antiparallel order, the spatial positioning of chromosome homologs was not perfectly symmetrical; comparison of the distribution of chromosome homologs on both sides of the rosette revealed variations in the spatial relations of chromosomes within each half of the rosette (Fig. 3F).
22. T. Freeman and R. Nagele, unpublished observations.
23. We used FISH and centromere-specific DNA probes to investigate spatial and temporal dynamics of centromere topology during the cell cycle in nuclei of HDFs. Before mitosis, centromeric subdomains began to aggregate into discrete centromere chains, each composed of several juxtaposed centromeres. Centromere chains appeared to merge into a single centromere ring that forms the hub of the prometaphase chromosome rosette. These coordinated movements of adjacent centromeric domains provide further indirect evidence that chromosomes may be attached to one another at the level of their centromeres (22).
24. HDFs were grown to high density confluence to arrest cells in the G<sub>1</sub> phase of the cell cycle in an effort to minimize cell cycle-dependent variations in chromosome topology. The cell cycle profiles of cultures and individual nuclei were obtained with a CAS 200 Cell Analysis System, which performs a Feulgen-based DNA quantitation. Cells were processed for FISH as described (12) with digoxigenin-labeled DNA probes for chromosomes 7, 8, 16, and X (13). Chromosomes 7, 8, and 16 were immediately adjacent to chromosome X in 46% ( $n = 181$ ), 49% ( $n = 119$ ), and 64% ( $n = 181$ ) of total nuclei, respectively (22). These results support a relation between the spatial positioning of specific chromosomes in the prometaphase rosette and that in the interphase nucleus.
25. HeLa and K562 erythroleukemia cells are both aneuploid, with the number of chromosomes ranging from 65 to 71 in >90% of cells. All chromosomes in these aneuploid cells appeared to be incorporated into a single chromosome rosette at prometaphase.
26. We thank K.-M. Lee and R. Carsia for helpful discussions, and N. Barlow from Micron Optics for help with microscopy.

9 June 1995; accepted 19 September 1995

## Diffusion Across the Nuclear Envelope Inhibited by Depletion of the Nuclear $\text{Ca}^{2+}$ Store

Lisa Stehno-Bittel,\* Carmen Perez-Terzic, David E. Clapham†

Intact, isolated nuclei and a nuclear membrane (ghost) preparation were used to study regulation of the movement of small molecules across the *Xenopus laevis* oocyte nuclear membrane. In contrast to models of the nuclear pore complex, which assume passive bidirectional diffusion of molecules less than 70 kilodaltons, diffusion of intermediate-sized molecules was regulated by the nuclear envelope calcium stores. After depletion of nuclear store calcium by inositol 1,4,5-trisphosphate or calcium chelators, fluorescent molecules conjugated to 10-kilodalton dextran were unable to enter the nucleus. Dye exclusion after calcium store depletion was not dependent on the nuclear matrix because it occurred in nuclear ghosts lacking nucleoplasm. Smaller molecules and ions (500-dalton Lucifer yellow and manganese) diffused freely into the core of the nuclear ghosts and intact nuclei even after calcium store depletion. Thus, depletion of the nuclear calcium store blocks diffusion of intermediate-sized molecules.

Eukaryotic cell nuclei are separated from the cytoplasm by a set of concentric lipid bilayers that form the nuclear envelope. The outer nuclear membrane and lumen of the envelope are continuous with endoplasmic reticulum (1). The transport of macromolecules and diffusion of smaller molecules and ions occurs through the nuclear pore complex (2), which traverses both nuclear membranes (3). Macromolecules greater than 70 kD require adenosine triphosphate (ATP) (4) and a nuclear localization sequence (NLS) (2, 5) to be transported. Smaller molecules containing an NLS also require ATP for their transport, but it is thought that there are no regulatory mechanisms for ions and molecules less than 40 to 70 kD that lack an NLS (6).

Inositol 1,4,5-trisphosphate ( $\text{InsP}_3$ ) releases  $\text{Ca}^{2+}$  from the nuclear envelope (7–9). Nuclear  $\text{InsP}_3$  channels have many of the same characteristics as endoplasmic reticular  $\text{InsP}_3$  channels (7, 8). Release of intracellular  $\text{Ca}^{2+}$  blocks transport of intermediate-sized molecules (10 kD) across the nuclear pore in situ (11). However,  $\text{Ca}^{2+}$  release initiates a cascade of events, and thus it is difficult to identify the components responsible for blocking transport across the nuclear envelope in intact cells. To directly assess this question, we developed methods to release  $\text{Ca}^{2+}$  from the nuclear store and simultaneously measure transport across the nuclear envelope in intact nuclei devoid of nucleoplasm.

Both the nucleoplasm and the lumen of the nuclear envelope (nuclear cisterna) have the potential to regulate  $\text{Ca}^{2+}$  inde-

pendently (12). Membrane-permeant forms of  $\text{Ca}^{2+}$ -sensitive dyes load the cisterna preferentially, whereas membrane-impermeant dyes monitor the concentration of  $\text{Ca}^{2+}$  ( $[\text{Ca}^{2+}]$ ) within the nucleoplasm (10). To avoid uncertainties when using small mammalian nuclei (2- to 3- $\mu\text{m}$  diameter), we used oocyte nuclei (~500- $\mu\text{m}$  diameter) to visualize the colocalization of the  $\text{Ca}^{2+}$  store and the nuclear envelope. Nuclei exposed to the membrane-impermeant form of fluo-3 fluoresced throughout the nucleoplasm but not in the region of the nuclear envelope (Fig. 1A). Membrane-permeant fluo-3 (fluo-3 AM) filled the nuclear cisterna as revealed by a thin fluorescent ring (Fig. 1B). The nuclear double membrane itself was defined by the membrane-specific dye rhodamine B ( $n = 6$ ). No fluorescence was detected in the central region of the nucleoplasm after exposure of the nucleus to fluo-3 AM, as determined by three-dimensional reconstruction of the entire nucleus ( $n = 3$ ).

$\text{Mn}^{2+}$  quenches  $\text{Ca}^{2+}$ -sensitive dye fluorescence (10) and can be used to monitor the flow of ions from the bath into the nuclear cisterna and nucleoplasm.  $\text{Mn}^{2+}$  (10  $\mu\text{M}$  to 1 mM) rapidly quenched nucleoplasmic fluorescence in nuclei loaded with the membrane-impermeant form of indo-1 ( $n = 15$ ) (Fig. 1C). In contrast to the rapid equilibration of  $\text{Mn}^{2+}$  into the nucleoplasm, fluorescence from the nuclear cisterna loaded with indo-1 AM was not altered by the addition of  $\text{Mn}^{2+}$  even after 30-min exposure to 10  $\mu\text{M}$   $\text{Mn}^{2+}$  ( $n = 5$ ) (Fig. 1D). To monitor  $\text{Mn}^{2+}$  flux into the nuclear cisterna, we loaded nuclei with both the membrane-permeant and impermeant forms of indo-1 ( $n = 3$ ). After the addition of  $\text{Mn}^{2+}$ , fluorescence from the center of the nucleus rapidly dissipated, leaving only the ring structure bounded by

Department of Pharmacology, Mayo Foundation, Rochester, MN 55905, USA.

\*Present address: University of Kansas Medical Center, 3901 Rainbow Boulevard, Kansas City, KS 66160–7601, USA.

†To whom correspondence should be addressed.